We are IntechOpen,
the world's leading publisher of
Open Access books
Built by scientists, for scientists

6,900
Open access books available

186,000
International authors and editors

200M
Downloads

154
Countries delivered to

Our authors are among the

TOP 1%
most cited scientists

12.2%
Contributors from top 500 universities

CLARIVATE ANALYTICS

BOOK CITATION INDEX

INDEXED

WEB OF SCIENCE™

Selection of our books indexed in the Book Citation Index
in Web of Science™ Core Collection (BKCI)

Interested in publishing with us?
Contact book.department@intechopen.com

Numbers displayed above are based on latest data collected.
For more information visit www.intechopen.com

GPS Modeling of the Ionosphere Using Computer Neural Networks

Daniel Okoh

Additional information is available at the end of the chapter

Abstract

This chapter presents a detailed description to modeling the ionosphere using the method of computer neural networks and data from the GPS (Global Positioning System). The chapter essentially motivates the use of artificial neural networks for ionospheric modeling, and it presents a detailed description of the processes and considerations involved in using artificial neural networks to model the ionosphere. Specific illustration was done using vertical total electron content (VTEC) data from 14 GPS stations in Nigeria that cover the period from years 2011 to 2016, to develop a neural network model of the GPS-TEC over Nigeria in space and in time. Sample simulations from the developed model shows that the model was accurate in predicting the VTEC variation patterns in terms of diurnal, seasonal, annual, longitudinal and latitudinal variations. A comparative analysis between the neural network predictions and those of other models like the IRI-Plas and NeQuick showed that predictions from the neural network model were predominantly more accurate.

Keywords: GPS, GNSS, TEC, neural network, ionosphere, model

1. Introduction

The ionosphere is important to our existence as it affects our radio communication systems, especially our satellite communication systems. Particularly, the ionosphere poses the greatest natural challenge for our global navigation satellite systems (GNSS) when it comes to precise position measurement by ground-based receivers. There are a couple of satellite navigation systems, e.g. the United States' GPS (Global Positioning System), Russia's GLONASS (Global Navigation Satellite System), European Union's GALILEO, China's

BEIDOU (or COMPASS), etc. The GPS is the most common and the most popular of the GNSS systems, and so in this chapter, we will carefully use the two words interchangeably. The evolution of our navigation requirements into satellite-based systems is therefore adding a rapid stair to interest in ionospheric research. The greatest efforts in ionospheric research have been directed towards ionospheric modeling, and related studies that tend to understand how the ionosphere changes in time and space. Several ionospheric models have been developed (e.g. Ref. [1–7]).

To understand exactly how the ionosphere influences our satellite-based navigation systems, it is important to understand how satellite-based navigation systems work. A more detailed introduction to the GNSS is presented by Ref. [8], but the core ideas are briefly and elegantly presented here. A satellite-based navigation system basically consists of some satellites in space. The satellites know their positions in space through the help of ground-based control stations and some internal programming. Through on-board transmitters on the satellites, each satellite continuously transmits radio signals. Each radio signal contains information about the 3-D position in space of the satellite from which it is transmitted, and the time in which the signal is transmitted. GPS receivers on ground (like the ones you and I own in cell phones and other devices) can receive these signals and automatically be able to compute the receivers' 3-D positions.

Exactly how does this happen? How does a GPS receiver know its position by merely receiving position and time stamped radio signals from the satellites? The GPS receivers use in-built computer programs to compute their own positions from the positions of the satellite they receive signals from. The computer programs are based on quite simple geometric calculations. The geometric calculations are based on the premise that if we know the exact 3-D positions of any three objects and the exact range to each of them, then we would be able to determine our own 3-D position. It is emphasized here that the positions of three objects are required because we are interested in 3-D positions. If we are interested in knowing our position in 2-D space, then we will require the positions of only two objects. In the case of the GPS, the interest is to know the 3-D position of the receiver as well as the time the signal is received (this makes 4-D), so we need four objects. A GPS receiver will therefore be able to compute its exact position and time if it receives signals from at least four satellites. From the satellite radio signals they receive, GPS receivers retrieve information on the 3-D positions and times of the satellites as well as the exact range to each of them.

As explained earlier, we know that each of the signals already contain information on the 3-D positions and times of the satellites, but how do the receivers know the ranges to the satellites? GPS receivers estimate ranges to the satellites by using the formula

$$\text{Range } = \text{ speed of radio signal} \times \text{travel time} \tag{1}$$

The travel time is how long the radio signals have traveled between their transmission and their reception (That is the time difference between when the signals were transmitted from the satellite and when they were received). The signals already contain information on when they were transmitted from the satellite, and the receiver time is one of the four parameters the receiver will compute.

The computation in Eq. (1) is based on the assumption that radio signals (which are electromagnetic) travel at the constant speed of about c = 2.998 × 10^8 ms^{-1} in vacuum. And this is where the problem of the ionosphere comes in. The space between the satellites and receivers is not entirely vacuum; there is an intervening region containing ionized matter known as the ionosphere. Because of ionized matter contained in the ionosphere, electromagnetic waves (e.g. the transmitted radio signals) do not travel through the ionosphere at the constant speed of about c = 2.998 × 10^8 ms^{-1}. The signals are delayed, and this delay is interpreted in Eq. (1) as part of the travel time. This introduces an error into the computed range (the computed range is greater than the actual or true range) which therefore subsequently manifests as an error in the computed receiver position.

An obviously intelligent thing to do is to remove this effect of the delay introduced by the ionosphere, but this is only possible if we know how much the delay is. To make the situation worse, the ionosphere is highly dynamic; it changes appreciably over space and time. We therefore need to know the extent of ionospheric ionization at any given time along the radio route so as to be able to correct for the effect of the ionosphere on the radio signal. This is where ionospheric models are useful. Ionospheric models can be used to now-cast (and even fore-cast) the extent of ionospheric ionization over space and time. And by so doing, ionospheric models are useful and usually applied in GPS error correction for single frequency receivers.

Single frequency receivers are GNSS receivers that can receive radio signals from the satellites in only one frequency. These are the most common types of GNSS receivers we see in everyday usage. They are cost-effective but incapable of estimating the ionospheric delay. On the other hand, there are dual or more frequency receivers which can receive GNSS radio signals at two or more frequencies. In the explanation that follows (on the Data and Methods section), dual or more frequency GNSS receivers are capable of estimating the ionospheric delays, and therefore capable of internally removing the effects of such delays. These types of receivers are mainly used for research and other specialized usages. It is from these types of receivers that data used in this chapter was obtained. There is general intuition that dual-frequency receivers are better than single frequency ones, but in highlighting the tradeoffs between the two, Ref. [9] explained that, asides cost effectiveness of the single frequency receivers, a single frequency receiver may actually outperform the more advanced dual-frequency receiver in terms of accuracy during the first 10 minutes or so, and also in places associated with frequent loss of lock on GNSS signals. Rather than using dual-frequency receivers, some applications therefore prefer using ionospheric models on single frequency receivers to correct for the effects of the ionosphere. The accuracy obtained from this practice however depends on the accuracy of the model used; more accurate models will give more accurate GNSS positions. The development of a regional GPS model of the ionosphere (with improved accuracy) is presented in this chapter. The modeling technique used is the method of computer neural networks.

Computer neural networks (also commonly referred to as neural networks or just NNs for short) have capability for machine learning as well as pattern recognition, and they have been demonstrated to be powerful tools for predictive modeling. NNs operate in a manner

that is similar to the human brain; the networks are composed of simple elements operating in parallel and inspired by the biological nervous system. NNs can learn trends and patterns in particular data they are given and consequently be able to correctly predict unseen and future trends for the data. A neural network can be trained to perform a particular function by adjusting the value of connections (also called weights) between elements [7]. The true power and advantages of neural networks lies in the ability to represent both linear and non-linear relationships directly from the data being modeled. Traditional linear models are simply inadequate when it comes for true modeling data that contains non-linear characteristics [8]. Recent explosion of ionospheric data from the GNSS is spurring interest in using computer neural networks for ionospheric modeling. A number of works have shown that neural networks (NNs) are good candidates for ionospheric modeling [6, 7, 10–13]. In this chapter, neural networks have been used to develop a regional model of the ionosphere over Nigeria. Predictions from the model have also been demonstrated to be more improved in terms of accuracy when compared to predictions from global ionospheric models like the IRI-Plas (International Reference Ionosphere—extended to the Plasmasphere) and the NeQuick.

2. Development of the GPS-based neural network model

2.1. Data and methods

Three main sets of data were used in this chapter, these include: (i) GPS data, (ii) sunspot number (SSN) data, and (iii) disturbance storm time (DST) data. The next section will dwell on GPS data which is of major interest in this chapter.

2.1.1. GPS data

The GPS data used in this chapter were derived from dual-frequency receivers on the NIGNET (Nigerian Permanent GNSS Network, www.nignet.net). A brief description of how ionospheric information is usually obtained from dual-frequency GPS receivers is presented.

How are dual-frequency GPS receivers able to estimate ionospheric delays? The delays introduced on radio signals by the ionosphere are frequency-dependent; the lower frequency signals are more delayed while the higher frequency signals are less delayed. More precisely, the delay (t) is inversely proportional to the radio frequency (f) as shown in Eq. (2a) [14].

$$t = 40.3 \times \frac{TEC}{cf^2} \qquad (2a)$$

c = 2.998 × 10⁸ ms⁻¹ is the speed of electromagnetic waves in vacuum, and TEC is the Total Electron Content. TEC is a parameter of the ionosphere that represents the total number of free electrons contained in a 1 m squared column, along the path of the signal through the ionosphere. It is this parameter of the ionosphere that is modeled in this chapter. Eq. (2a) shows that the ionospheric delay is directly proportional to the TEC, therefore the radio signals are more delayed when they travel through a route in the ionosphere with more number of free electrons.

The proportionality expressed in Eq. (2a) forms the underlying principle for deriving ionospheric information (precisely TEC) using dual-frequency GPS receivers. This is because two radio signals (having frequencies, f_1 and f_2) transmitted at the same time from the same satellite will be delayed differently by the ionosphere so they arrive the same receiver at different times. The delays that will be experienced by the two radio signals are, respectively, given by Eq. (2b) and Eq. (2c).

$$t_1 = 40.3 \times \frac{TEC}{c f_1^2} \tag{2b}$$

$$t_2 = 40.3 \times \frac{TEC}{c f_2^2} \tag{2c}$$

Subtracting Eq. (2b) from Eq. (2c), we get the time delay between arrivals of the two signals as in Eq. (3a).

$$\Delta t = t_2 - t_1 = \frac{40.3\, TEC}{c}\left(\frac{1}{f_2^2} - \frac{1}{f_1^2}\right) \tag{3a}$$

Dual-frequency GPS receivers compute the TEC using Eq. (3b) which is obtained by making TEC subject of the formula from Eq. (3a).

$$TEC = \frac{c\,\Delta t}{40.3\left(\frac{1}{f_2^2} - \frac{1}{f_1^2}\right)} \tag{3b}$$

The TECs computed in this manner using the pseudo-range measurements alone are usually noisy; differential carrier phase measurements are used to obtain precise measures of the relative TECs, and a combination with the pseudo-range measurements provide the absolute slant TEC values (STECs) along the receiver-satellite path [15–17]. The computed TECs are referred to as slant, to distinguish them from the unique TEC that will be obtained for a particular location when the satellite is exactly overhead the location (that is, satellite elevation = 90°). This unique TEC is called the vertical TEC (VTEC). VTECs are usually derived from the STECs using Eq. (4).

$$VTEC = \frac{STEC - (b_r + b_s)}{S(E)} \tag{4}$$

where br and bs are, respectively, the receiver and satellite biases, S(E) is the mapping function defined by Eq. (5) [18].

$$S(E) = \frac{1}{\cos(z)} = \left[1 - \left(\frac{R_E \times \cos(E)}{R_E + h_s}\right)^2\right]^{-\frac{1}{2}} \tag{5}$$

z and E are, respectively, the zenith and elevation angles in degrees; R_E and h_s are, respectively, the mean Earth radius and the ionosphere (effective) height above the Earth surface in km. The value of h_s used for this chapter is 350 km.

GPS Data obtained from the NIGNET are in RINEX (Receiver Independent Exchange) format. The RINEX format is the standard data interchange format for raw satellite navigation system data. RINEX format data obtained from the NIGNET were processed into VTEC data using software developed by Dr. Gopi Seemala (seemala.blogspot.in). The software works basically on the principles highlighted above, and as expressed in Refs. [15, 19].

GPS Data used were from the 14 stations illustrated in **Figure 1** and in **Table 1**. All available data coving the periods from years 2011 to 2016 were used. To obtain instantaneous values of VTEC for a given location, VTEC values from the various satellites that are visible over the location at the time were averaged excluding those from satellites with elevation angles less than 25°. The reason for excluding data associated with low elevation angles is usually to minimize multipath errors. Multipath errors are errors associated with signals that bounce off (or reflected from) nearby buildings, trees, or other structures before they reach the receiver antenna. The problem with these signals is that the resulting range will be greater than the actual straight path range between the satellite and receiver, because the signal first has to bounce off other structures before they reach the receiver antenna. The multipath problem is typical of signals coming from low elevation satellites; the lower the satellite elevation angles (especially satellites close to the horizon), the more likely signals from them are to bouncing
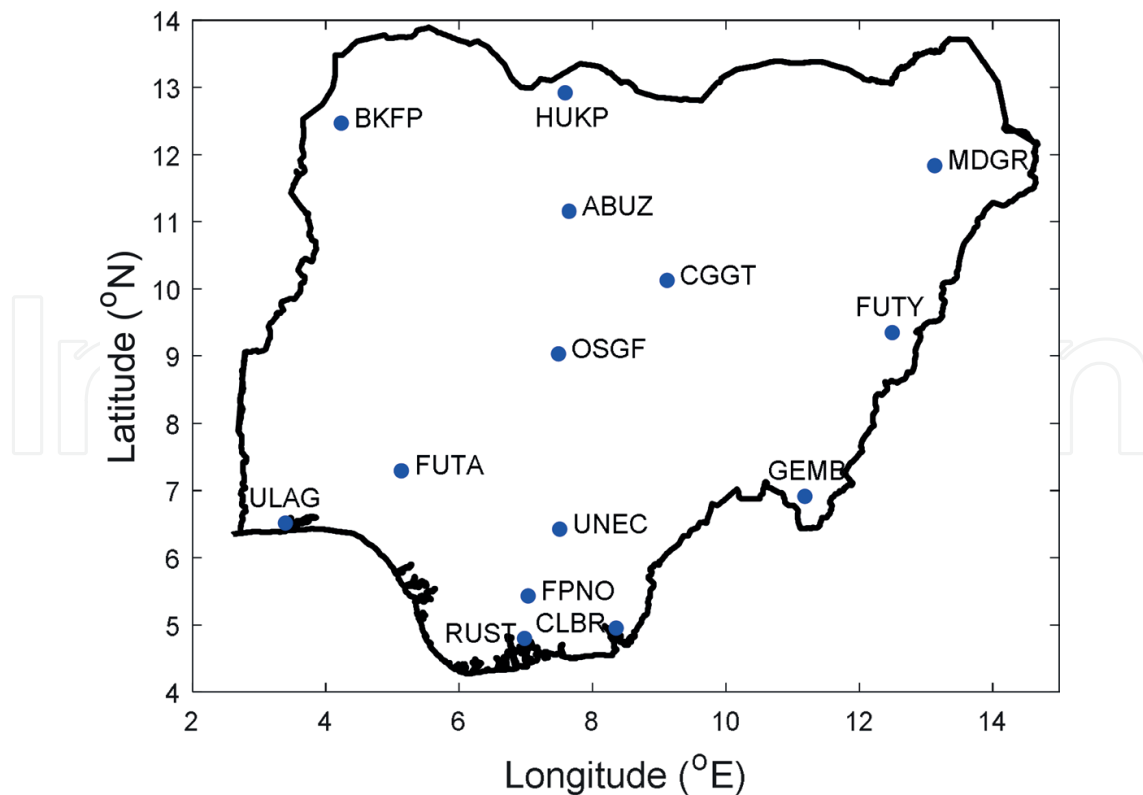

Figure 1. Map of Nigeria showing locations of GPS stations used in this work.

Station Code	City	State	Latitude (deg)	Longitude (deg)	Elevation (m)
ABUZ	Zaria	Kaduna	11.1517	7.6486	706.1
BKFP	Birnin-Kebbi	Kebbi	12.4684	4.2292	251.0
CGGT	Toro	Bauchi	10.1231	9.1181	917.4
CLBR	Calabar	Cross-River	4.9503	8.3514	61.5
FPNO	Owerri	Imo	5.4345	7.0331	92.6
FUTA	Akure	Ondo	7.2986	5.1364	416.0
FUTY	Yola	Adamawa	9.3497	12.4978	248.4
GEMB	Gembu	Taraba	6.9170	11.1839	1796.6
HUKP	Katsina	Katsina	12.9211	7.5909	565.0
MDGR	Maiduguri	Borno	11.8381	13.1309	351.8
OSGF	Abuja	Federal-District	9.0275	7.4861	533.6
RUST	Port-Harcourt	Rivers	4.8017	6.9784	46.6
ULAG	Lagos	Lagos	6.5172	3.3975	45.5
UNEC	Enugu	Enugu	6.4247	7.5047	255.4

Table 1. Description of NIGNET stations used in this work.

off other structures before they reach the receiver antenna. This problem is mostly the reason why research-class GNSS receivers are installed such that their antennas are raised above nearby structures/buildings (or away from the structures/buildings), and the antennas are built in such a shape that the receiving surface faces the sky. In this way, radio signals that are reflected from structures beneath the antenna do not get received by the antenna even when they hit the bottom surface of the antenna. The resulting VTEC data were further averaged in 1-hour intervals to reduce data and to lessen spikes on the data profiles.

2.1.2. Other data

The other two set of data used in this chapter are the DST and SSN data. The DST is a measure of the disturbances in the Earth's magnetic field, it is an index often used to describe the level of geomagnetic activity during storms. On the other hand, the SSN is a count of the number of sunspots present on the surface of the Sun. It is a measure of the Sun's activeness (the level of activity going on in the Sun), and is found to be cyclical, reaching its peak in about every 11 years.

The idea in formulating the input layer structure of a neural network is to consider parameters/factors that affect the output parameter (which is VTEC in this chapter). VTEC has been convincingly proven to be affected by both geomagnetic storm activity [20] and solar activity [21]. The practice in neural networks is to supply parameters like DST and SSN which are

well established to affect VTEC as inputs during the training of a network that will predict VTEC. For this reason, the DST and SSN parameters corresponding to instances of the VTEC data used in this chapter were used as inputs during the training of the neural networks in this chapter.

DST indices were obtained from the World Data Center (WDC) for Geomagnetism (http://wdc.kugi.kyoto-u.ac.jp/dstdir/index.html), while data on SSN were obtained from the WDC-SILSO (Sunspot Index and Long-term Solar Observations, http://www.sidc.be/silso/datafiles), Royal Observatory of Belgium, Brussels.

2.1.3. Neural network training and testing

The Levenberg-Marquardt back-propagation algorithm [22] as implemented in MATLAB was used in this chapter. A couple of other algorithms exist [23] but the Levenberg-Marquardt algorithm is admired for its speed and efficiency in learning [24, 25]. NNs typically have input layers, output layers, and intermediary hidden layers. Each layer could consist of one or more units or nodes (also called neurons).

As explained in the previous section, the idea in formulating the input layer structure of a neural network is to consider parameters/factors that affect the output parameter. In the previous section, the inclusion of DST and SSN as inputs was justified. Other factors that have been established to affect VTEC are time and space; VTEC is known to vary with time and space.

Particularly, VTEC changes with time in the forms of diurnal, seasonal, and long-term yearly variations [7]. For the neural networks to learn long-term yearly variations, the year for each of the GPS VTEC data was included as input for the training. To learn seasonal variations, the day of the year for each of the data was included, and to learn diurnal variations, the hour of day for each data was included.

Spatially, VTEC changes with longitude and latitude of the GPS receiver location, and so the longitudes and latitudes of the GPS receivers were included for each of the GPS VTEC data so that the networks will learn spatial variations of the VTEC. Geomagnetic longitudes and latitudes (rather than geographic longitudes and latitudes) were used since the ionospheric properties are based mainly on the interactions between the solar radiation and the Earth's geomagnetic field [6, 26]. Conversion of geographic to geomagnetic coordinates was done using the Apex Coordinate Conversion Utility Software [27].

In summary, a total of the following seven input nodes were used for the neural network training:

1. Hour of Day (to learn diurnal variations of the VTEC)

2. Day of Year (to learn the seasonal variations)

3. Year (to learn the long-term yearly variations)

4. Longitude (to learn the spatial variations longitude-wise)

5. Latitude (to learn the spatial variations latitude-wise)

6. DST index (to learn variations of the VTEC with geomagnetic storm activity)

7. SSN (to learn variations of the VTEC with solar activity)

The output layer is clearly known to have one neuron which is the GPS-VTEC to be modeled, but deciding the number of neurons in the hidden layer is an intricate aspect of neural network trainings. This is an aspect that conspicuously affects the performance of the trained networks. The most credible practice to deciding an appropriate number of hidden layer neurons has been to train several networks that vary in the number of hidden layer neurons, and then selecting the best of them using a performance index.

In this chapter, 20 neural networks were simulated, varying the number of hidden layer neurons in integer steps from 1 to 20. The main performance index used is the root-mean-squared-errors (RMSEs). RMSEs were computed using the formula in Eq. (6).

$$\text{RMSE} = \sqrt{\frac{\sum\limits_{i=1}^{n}(\text{GPSVTEC}_i - \text{NNV TEC}_i)^2}{n}} \tag{6}$$

where GPSVTEC_i and NNVTEC_i NNVTEC_i are, respectively, the GPS-VTEC values and the NN-predicted VTEC values, n is the number of samples predicted.

The criteria for deciding the best network is to choose the one that gives the least RMSE on the test dataset. Testing of the networks was done using 15% dataset that was randomly selected from the entire data and which were not used for the training. Another randomly selected 15% of the data was used for validation during the training, and the remaining 70% was used for the actual training. **Figure 2** illustrates outcomes of the RMSEs when different number of hidden layer neurons were used on the networks.

Figure 2 shows that the network that gave the least RMSE is the network that has 6 hidden layer neurons. The RMSE for this network is 5.03 TECU. It is this network that has been adopted as the optimal network in this study. A detailed and elementary treatment on how to train neural networks using MATLAB is contained in a more elementary book [28].

2.2. Results and discussions

2.2.1. Sample simulations

Using the Neural Network model developed in this chapter, sample simulations were made to assess predictions from the model in terms of known ionospheric variation patterns.

2.2.1.1. Diurnal variations

Diurnal variations of the ionosphere are variations in the ionosphere that are observed as the Earth makes a complete rotation about its axis. That is, the changes that are observed within an entire day as we go from morning to night. **Figure 3(a)–(d)** are constructed to visualize
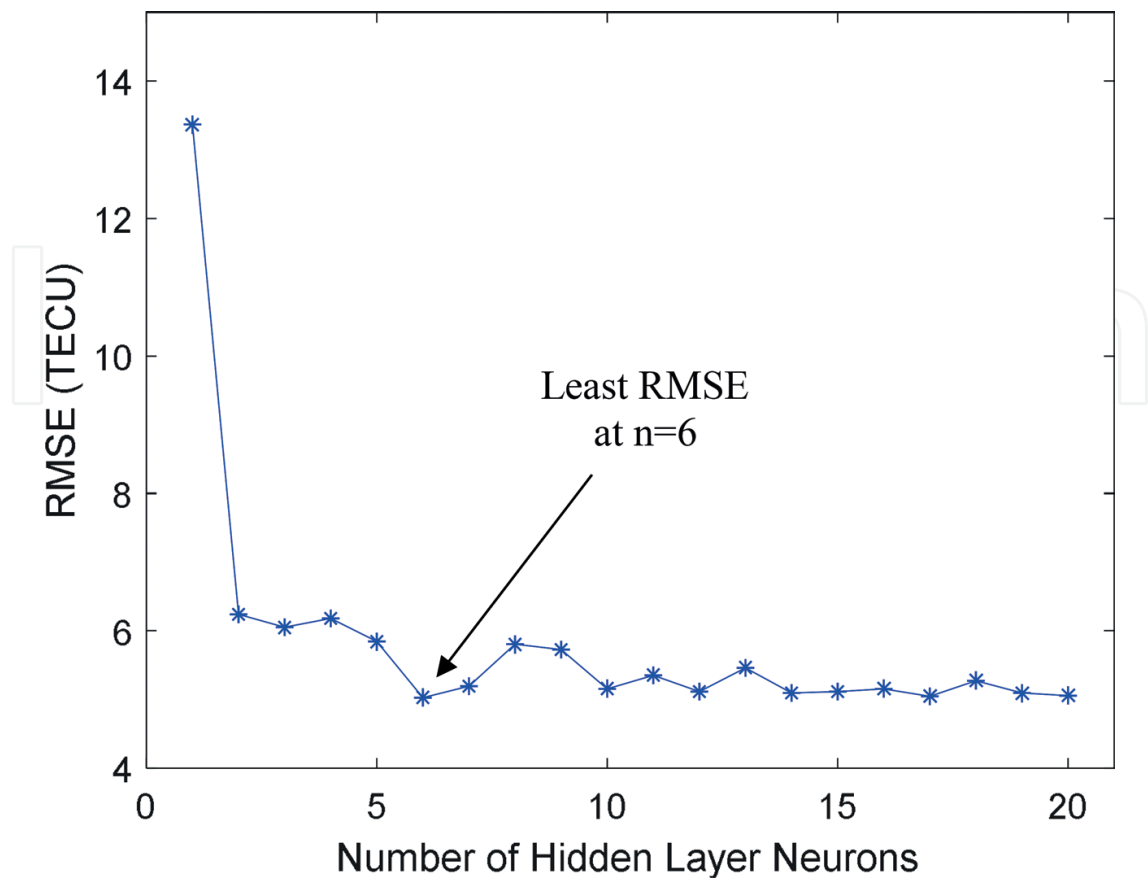
Figure 2. Plot of the RMSEs for varied number of hidden layer neurons.

diurnal variations in the ionosphere over the Nigerian region. The figures are, respectively, images of the VTEC over Nigeria for 05:00 UT (06:00 local Nigerian time, which is around local sunrise), 11:00 UT (12:00 local Nigerian time, which is around local midday), 17:00 UT (18:00 local Nigerian time, which is around local sunset), and 23:00 UT (24:00 local Nigerian time, which is around local midnight) of 1st July 2014. The day was arbitrarily chosen for this illustration. Local time in Nigeria is UT + 1. In the color scheme used for the figure (and for all other figures in this chapter), the blue colors indicate lower VTECs, the red colors indicate higher VTECs, and the green-yellow colors indicate moderate VTECs (see the associated color bars for exact VTEC values in each case).

Figure 3 shows that within a day the VTEC values are greatest around local midday. Since the Sun is the major source of ionospheric ionization, the level of ionospheric ionization (and hence VTEC value) is usually higher during the daytime (when the solar-zenith angle is low) than at nights (when the solar-zenith angle is high). The VTEC values are also relatively high around sunset because the ionizations produced by the Sunlight do not instantly disappear (it takes about 2 hours for the ionized particles to substantially recombine when the Sun goes below horizon).

Figure 3(a) and **(c)** also reveals the interplay between the Sun and the ionosphere during sunrise and sunset. At sunrise (**Figure 3(a)**), the VTECs are higher eastwards than westwards.
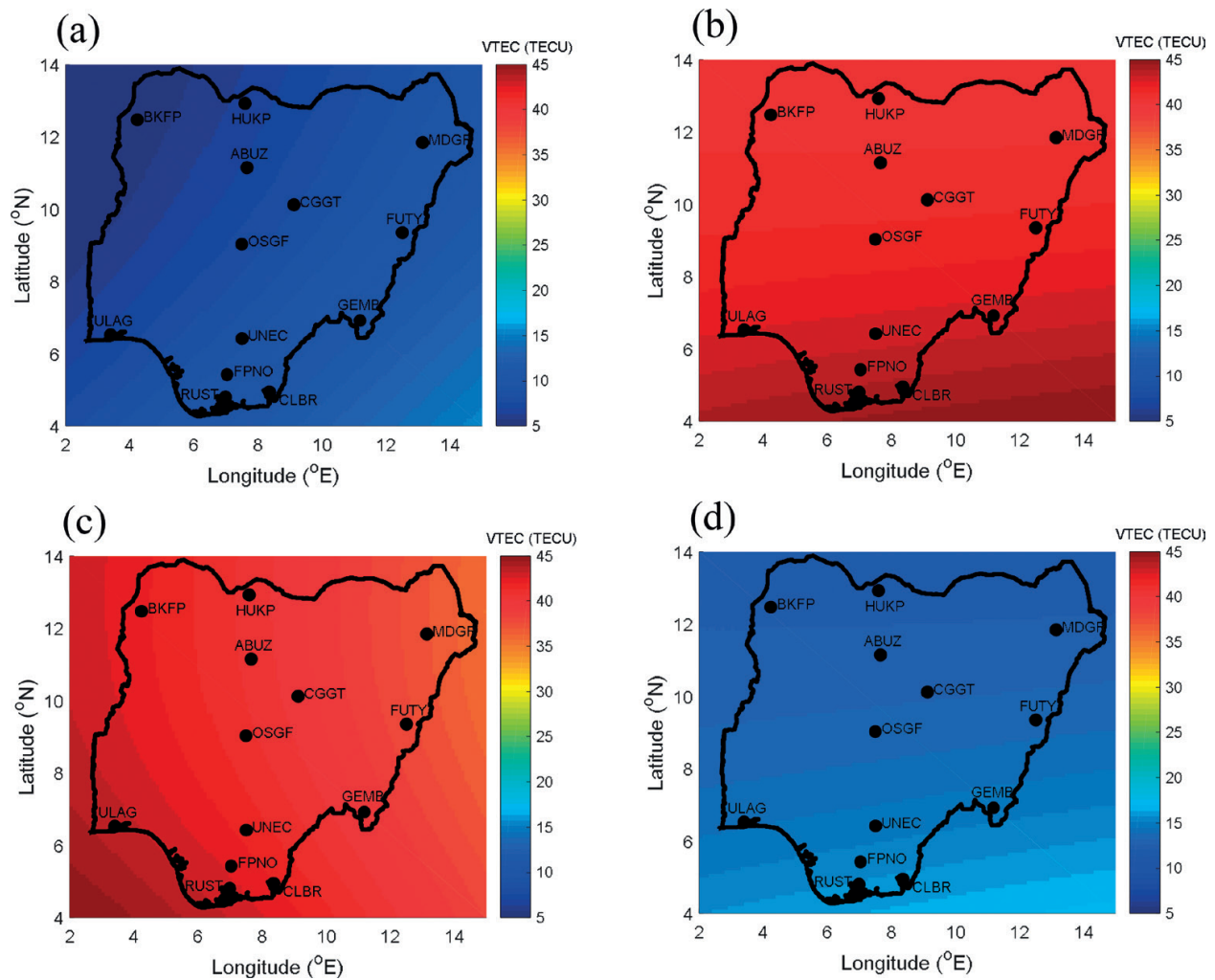
Figure 3. VTEC maps over Nigeria for (a) 06:00 LT, (b) 12:00 LT, (c) 18:00 LT, and (d) 24:00 LT, of 1st July 2014.

This is because the Sun rises from the east. At sunset (**Figure 3(c)**), the VTECs are higher westwards than eastwards. This is because the Sun sets to the west.

2.2.1.2. Seasonal variations

Seasonal variations have to with variations that are observed as the Earth makes a complete revolution about the Sun. That is, the changes that are observed within an entire year as we go through the seasons. **Figure 4(a)–(d)** are constructed to illustrate seasonal variations over Nigeria during year 2012. The figures are, respectively, VTEC maps of the Nigerian region for 11:00 UT (local midday) of 20th March 2012 (the March equinox day), 21st June 2012 (the June solstice day), 22nd September 2012 (the September equinox day), and 21st December 2012 (the December solstice day). The year 2012 was arbitrarily chosen for the illustration.

Figure 4(a) and **(c)** illustrates that the VTECs are relatively high during the equinoxes. This is because Nigeria is located close to the equator, and as such receives much sunlight during the

equinoxes. During the equinoxes, the solar-zenith angle is lower at the equator as compared to the solstices. It is also conspicuous that the VTEC values are high during the December solstice (**Figure 4(d)**), even higher than at the September equinox (**Figure 4(c)**). This is because Nigeria is mostly located on the geomagnetic southern hemisphere. The December solstice is the summer solstice in the southern hemisphere, and so the solar-zenith angle is lower in the southern hemisphere during this season than at other seasons.

2.2.1.3. Long-term solar cycle variations

The ionosphere has also been established to vary with the level of solar activity. As explained earlier, the sunspot number is a good measure of the level of solar activity. The solar activity is known to have a time series cycle of about 11-years during which the activity level goes from peak to peak or trough to trough.
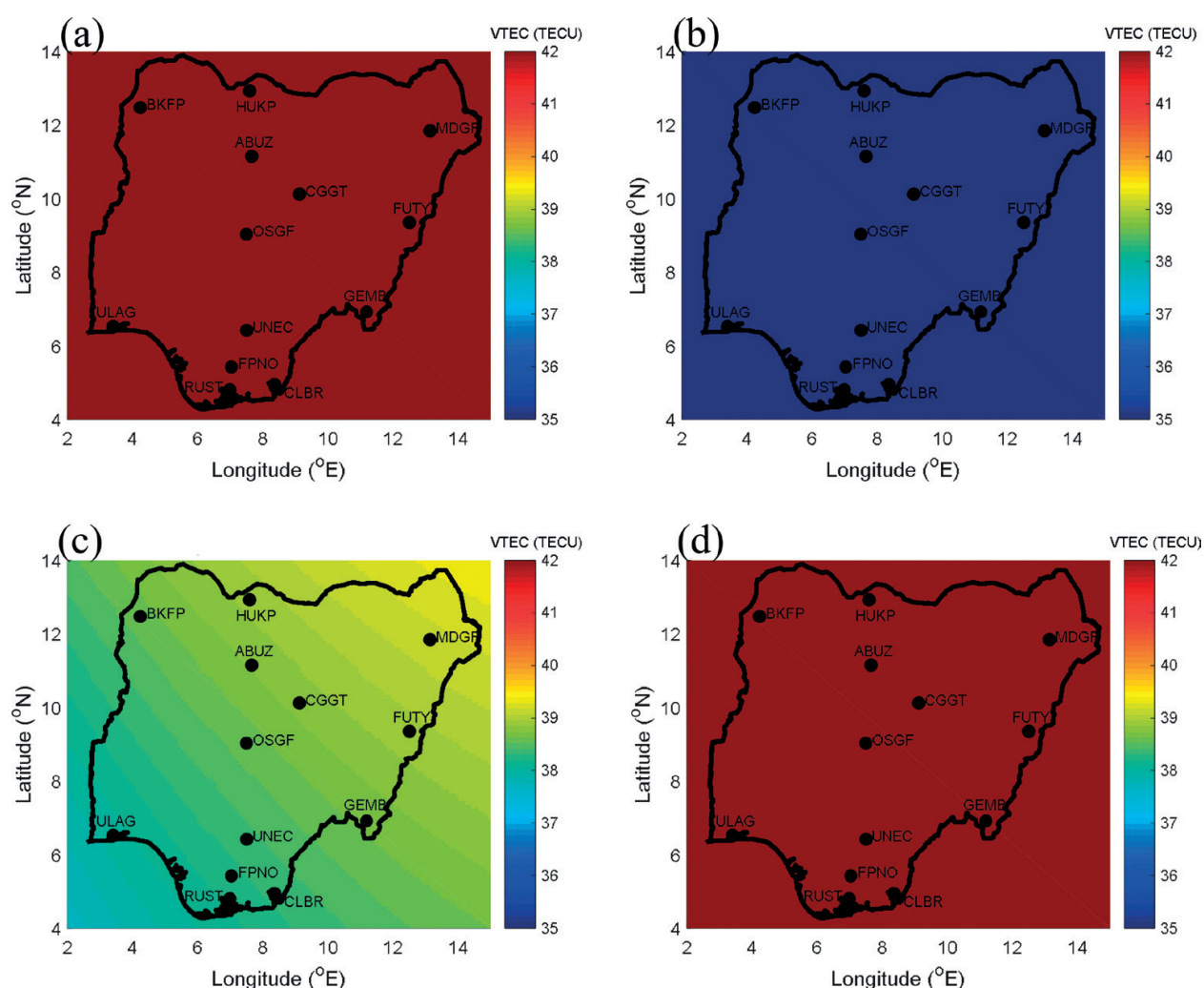
Figure 4. VTEC maps over Nigeria for local midday of (a) 20th March, (b) 21st June, (c) 22nd September, and (d) 21st December, of year 2012.

Figure 5(a)–(d) was constructed to illustrate how the ionosphere over Nigeria varies with the solar activity. The figures are, respectively, the local midday VTECs over Nigeria for the same day (1st July) of years 2011, 2012, 2013, and 2014.

A look at the solar activity cycle shows that the solar activity level was on the rise from year 2011 to year 2014. Comparing with the VTEC values for those years (**Figure 5(a)–(d)**), it is observed that the VTEC values are also on the increase; the VTECs are least during year 2011 (**Figure 5(a)**) which also has the least solar activity level, and greatest during year 2014 (**Figure 5(d)**) which also has the greatest solar activity level. **Figure 5(a)–(d)** clearly indicates that the neural network was able to learn/capture the long-term variations associated with the solar activity.

2.2.2. Comparison of neural network predictions with IRI-Plas and NeQuick predictions

Two of the most popular global ionospheric models (the IRI-Plas and the NeQuick) have been selected to make a comparative assessment of the neural network model developed in this chapter.
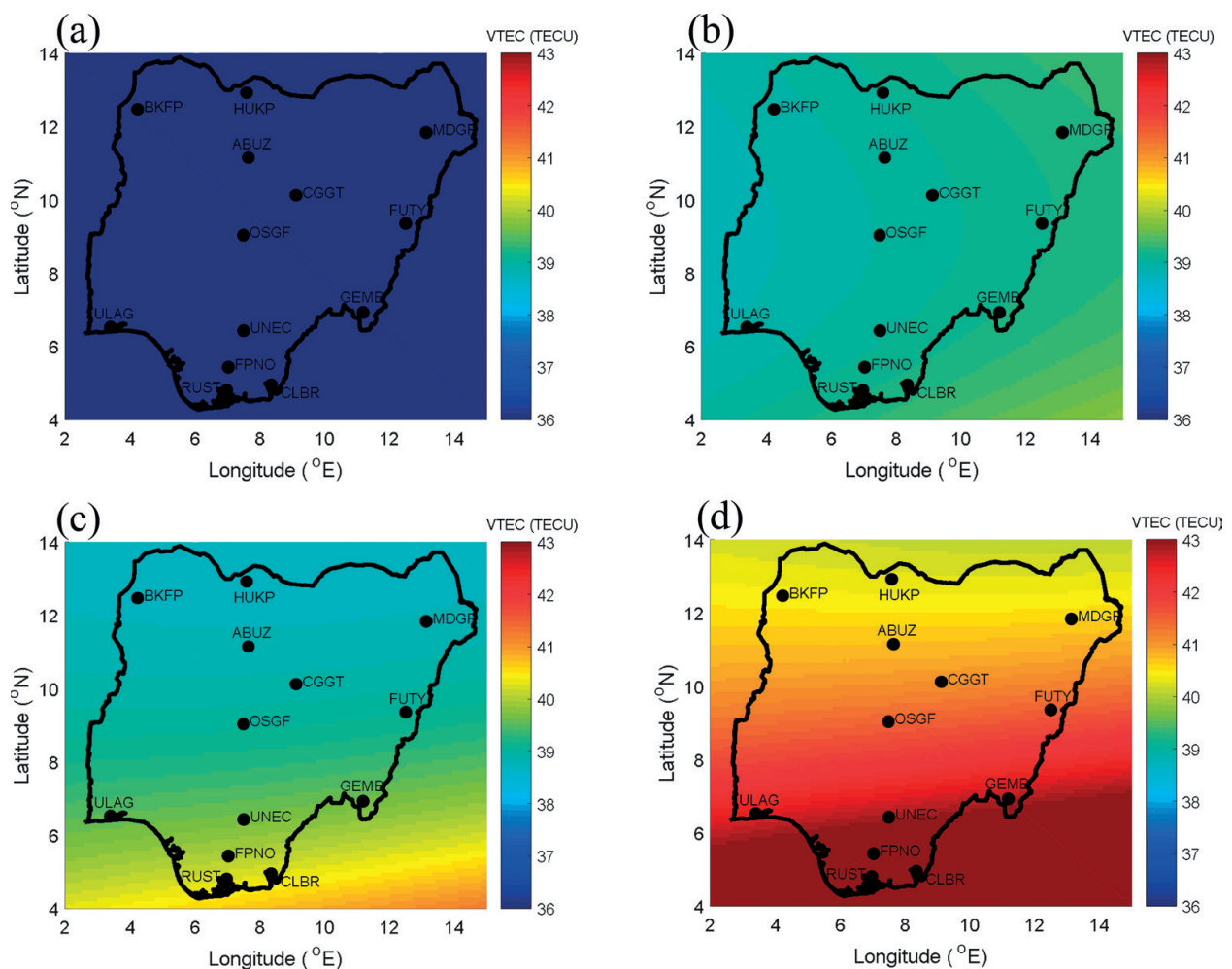

Figure 5. VTEC maps over Nigeria for local midday of 1st July, year (a) 2011, (b) 2012, (c) 2013, and (d) 2014.

The IRI-Plas is the IRI (International Reference Ionosphere) extended to the plasmasphere [29]. The IRI model [3] has been widely accepted as a defector standard for specifying ionospheric parameters across the globe. The IRI-Plas model (rather than the IRI model) is selected for use in this chapter because TEC computed by the IRI-Plas model involves electron density integrations up to the GPS satellite altitudes of about 20,200 km, whereas for the IRI model, it only gets up to a maximum of 2000 km. Since, this chapter concentrates on TEC derived from the GPS, a more comprehensive comparison is therefore obtained using the IRI-Plas model rather than the IRI model. The IRI-Plas model has also been proposed for extension of the IRI model to the plasmasphere [30]. The most recent version of the IRI-Plas (the IRI-Plas 2017) was used for this comparison. The windows executable program of the IRI-Plas used was obtained from the website of the IZMIRAN Institute (http://ftp.izmiran.ru/pub/izmiran/SPIM/).

The NeQuick [31–33] is another popular global ionospheric model which has been severally compared with GNSS TEC measurements and shown to be a good representation of the
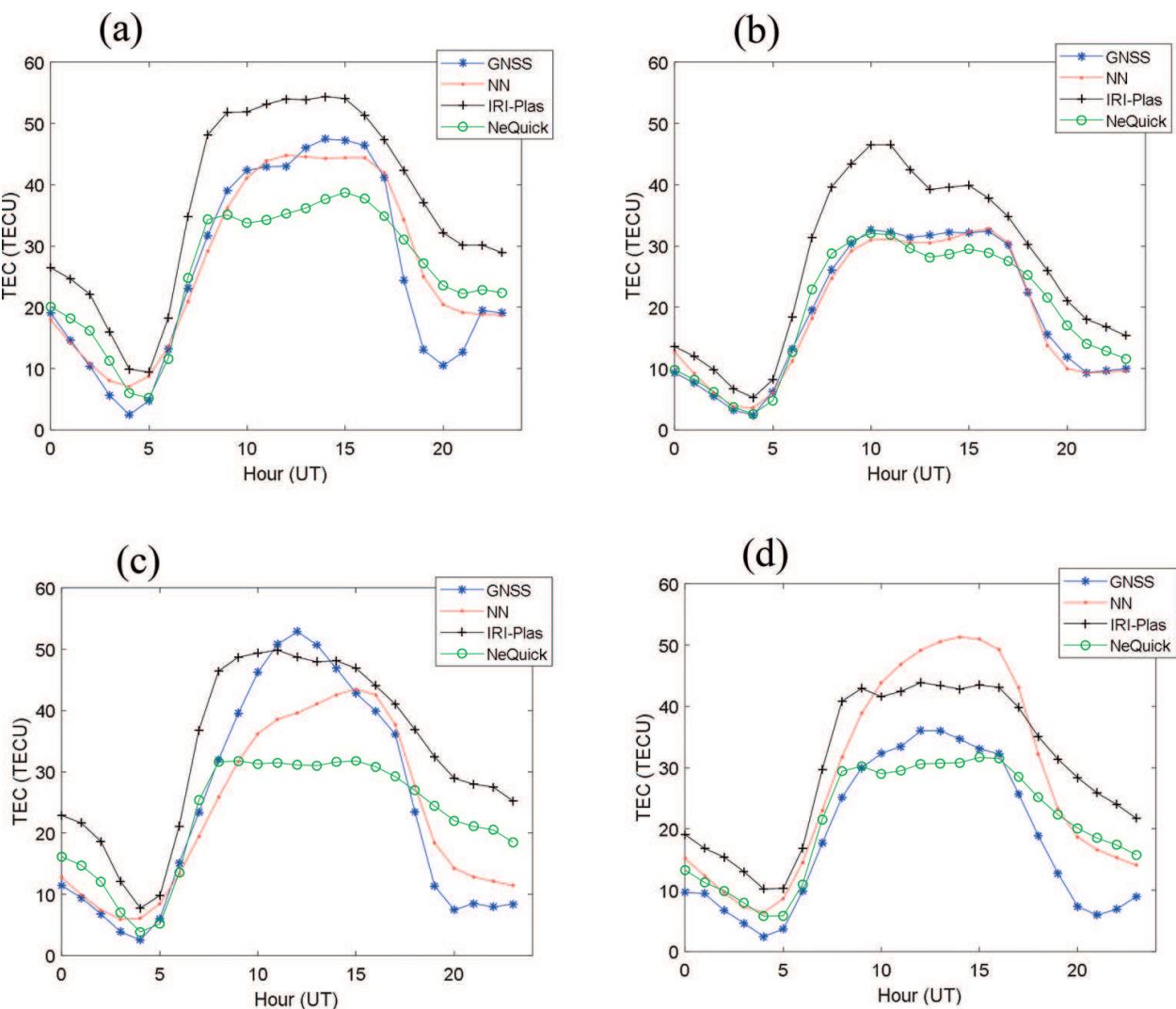

Figure 6. Diurnal VTEC plots over the OSGF stations for days of (a) March Equinox, (b) June Solstice, (c) September Equinox, and (d) December Solstice, in year 2012.

	NN	IRI-Plas	NeQuick
March Equinox	4.4544	12.0488	7.1809
June Solstice	1.2941	8.5256	2.7717
September Equinox	5.9616	11.6634	11.0269
December Solstice	10.7685	12.3848	5.8034

Table 2. Diurnal RMSEs of the 3 models for the days illustrated in **Figure 6**.

ionosphere. The NeQuick is admired because of its improved performance in predicting the topside ionosphere, and consequently versions of the IRI model from 2007 and later have included the topside formulation of the NeQuick, and has adopted it as the most mature of the different proposals to compute the topside part of the IRI electron density profile [33, 34]. The NeQuick includes routines that compute the electron density along any ray-path from ground to GPS satellite altitudes of about 20,200 km, and so also makes for a comprehensive comparison with observations from the GPS. The latest version of the NeQuick (the NeQuick-2, which is currently recommended by the ITU [35] is the one used for this comparison. The NeQuick-2 used in this chapter is the windows executable program created from the FORTRAN source code, and was obtained from the Ionosphere Radio propagation Unit of the T/ICT4D Laboratory (https://t-ict4d.ictp.it/nequick2/source-code).

For the purpose of visual illustration, the diurnal VTEC profiles from GPS observations for four selected days, over the OSGF station, are illustrated in **Figure 6(a)–(d)** alongside corresponding VTEC predictions from the NeQuick, the IRI-Plas model, and the neural network (NN) model developed in this chapter. **Figure 6(a)–(d)**, respectively, represents diurnal VTEC profiles over the OSGF station for 20th March 2012 (the March equinox day), 21st June 2012 (the June solstice day), 22nd September 2012 (the September equinox day), and 21st December 2012 (the December solstice day).

Figure 6 clearly indicates that the VTEC predictions from the NN model developed in this chapter were closer to the GPS VTEC observations in most of the times than the VTEC predictions of the IRI-Plas and NeQuick. **Table 2** summarizes the RMSEs (computed using Eq. (6)) for each of the days and models illustrated in **Figure 6**. The RMSEs for each of the models were computed with reference to the GPS observations. **Table 2** shows that the prediction errors for the NN model were predominantly lower than for the other two models, except for the December solstice day when the NeQuick prediction error was lower.

Asides the demonstrated capability of neural networks to very accurately learn and predict variations in the ionosphere, the better performance of the NN model could also be linked to the fact that more volume of regional GPS data (GPS data from the Nigerian region) were used in the NN model than the volume used in either of the NeQuick or IRI-Plas models.

3. Conclusion

A regional VTEC model over Nigeria was developed using the method of computer neural networks and GPS-VTEC data from 14 stations spanning the period from years 2011 to 2016. A total of seven input layer neurons (namely, Year, Day of Year, Hour of Day, Geomagnetic Longitude, Geomagnetic Latitude, SSN, and DST indices) were used to learn the studied output (GPS-TEC). By simulating 20 different networks that differed in their number of hidden layer neurons, the network with 6 hidden layer neuron was determined to be the best in terms of minimizing the prediction errors (using the RMSE as criterion for measuring the prediction error).

The neural network model was demonstrated to be proficient in predicting the VTEC variation patterns in terms of diurnal variations, seasonal variations, long-term solar cycle variations, and spatial variations across Nigeria.

When compared with two popular global ionospheric models (the NeQuick and the IRI-Plas), predictions from the neural network model was observed to be more accurate in terms of closeness to the GPS-VTEC values. Typical RMSEs for the neural network model predictions were between 1.3 and 10.8 TECU, the mean RMSE was 5.6 TECU. For the IRI-Plas model, the RMSEs were between 8.5 and 12.4 TECU, and the mean was 11.2 TECU. For the NeQuick, the RMSEs were between 2.8 and 11.0 TECU, and the mean was 6.7 TECU. The work done in this chapter further validates neural networks as excellent candidates for modeling of ionospheric parameters.

Acknowledgements

Author details

Daniel Okoh

Address all correspondence to: okodan2003@gmail.com

Space Environment Research Laboratory, Centre for Atmospheric Research, National Space Research and Development Agency, Abuja, Nigeria

References

[1] Chiu YT. An improved phenomenological model of ionospheric density. Journal of Atmospheric and Terrestrial Physics. 1975;**37**:1563-1570

[2] Roble RG, Ridley EC, Richmond AD. A coupled thermosphere/ionosphere general circulation model. Geophysical Research Letters. 1988;**15**(12):1325-1328

[3] Bilitza D. International Reference Ionosphere 1990. Greenbelt Maryland: National Space Science Data Center 90-22; 1990

[4] Bailey GJ, Balan N, Su YZ. The Sheffield University plasmasphere ionosphere model-a review. Journal of Atmospheric and Solar - Terrestrial Physics. 1997;**59**(13):1541-1552

[5] Huba JD, Joyce G, Fedder JA. Sami2 is another model of the ionosphere (SAMI2) - a new low-latitude ionosphere model. Journal of Geophysical Research. 2000;**105**(A10): 23035-23053

[6] Habarulema JB. A contribution to TEC modelling over Southern Africa using GPS data [PhD Thesis]. Rhodes University; 2010

[7] Okoh D, Owolabi O, Ekechukwu C, Folarin O, Arhiwo G, Agbo J, Bolaji S, Rabiu B. A regional GNSS-VTEC model over Nigeria using neural networks: A novel approach. Geod Geodyn. 2016;**7**(1):19-31

[8] NovAtel, An Introduction to GNSS [Internet]. 2010. Available from: http://www.borealisprecision.com/pdf/An_Introduction_to_GNSS.pdf [Accessed: 2017-12-07]

[9] Marel HVD, Bakker PFD. Single versus Dual Frequency Precise Point Positioning. GNSS Solutions, in InsideGNSS [Internet]. 2012. Available from: www.insidegnss.com/auto/julyaug12-Solutions.pdf [Accessed: 2017-12-11]

[10] Leandro RF, Santos MC. A neural network approach for regional vertical total electron content modeling. Studia Geophysica et Geodaetica. 2007;**51**:279-292

[11] Hernandez-Pajares M, Juan J, Sanz J. Neural network modeling of the ionospheric electron content at global scale using GPS. Radio Science. 1997;**32**:1081-1090

[12] Tulunay E, Senalp ET, Cander LR, Tulunay YK, Bilge AH, Mizrahi E, et al. Development of algorithms and software for forecasting, nowcasting and variability of TEC. Annales de Geophysique. 2004;**47**:1201-1214

[13] Senalp ET, Tulunay E, Tulunay Y. Total electron content (TEC) forecasting by Cascade modeling, a possible alternative to the IRI-2001. Radio Science. 2008;**43**:RS4016. DOI: 10.1029/2007RS003719.2008

[14] Klobuchar JA. Ionospheric effects on GPS. In: Parkinson BW, Spilker JJ, editors. Global Positioning System: Theory and Applications, Vol. 2. Progress in Astronautics and Aeronautics. 1996. p. 164

[15] Rao PVS, Gopi KS, Niranjan K, Prasad SVVD. Temporal and spatial variations in TEC using simultaneous measurements from the Indian network of receivers during the low solar activity period of 2004-2005. Annales de Geophysique. 2006;**24**:3279-3292

[16] Jin SG, Occhipinti G, Jin R. GNSS ionospheric seismology: Recent observation evidences and characteristics. Earth Science Reviews. 2015;**147**:54-64

[17] Zhu FY, Wu Y, Lin J, Zhou Y. Temporal and spatial characteristics of VTEC anomalies before Wenchuan Ms8.0 earthquake. Geodesy and Geodynamics. 2010;**1**(1):23-28

[18] Mannucci AJ, Wilson BD, Edwards CD A new method for monitoring the earth's iono-spheric total electron content using the GPS global network. In: Proc. of ION GPS-93. Inst Navigation; 1993. pp. 1323-1332

[19] Seemala GK, Valladares CE. Statistics of total electron content depletions observed over the south American continent for the year 2008. Radio Science. 2011;**46**:RS5019. DOI: 10.1029/2011RS004722

[20] Malik R, Sarkar S, Mukherjee S, Gwal AK. Study of ionospheric variability during geo-magnetic storms. Journal of Indian Geophysical Union. 2010;**14**(1):47-56

[21] Correia E, Paz AJ, Gende MA. Characterization of GPS total electron content (GPS-TEC) in Antarctica from 2004 to 2011. Annals of Geophysics. 2013;**56**(2):R0217

[22] Levenberg K. A method for the solution of certain nonlinear problems in least squares. Quarterly of Applied Mathematics. 1944;**2**:164-168

[23] Quesada AA. Five Algorithms to train a neural network [Internet]. 2017. Available from: https://www.neuraldesigner.com/blog/5_algorithms_to_train_a_neural_network [Accessed: 2017-12-07]

[24] Demuth H, Beale M. Neural Network Toolbox for Use with MATLAB. Natick, MA, USA: Mathworks Inc; 2002

[25] Kisi O, Uncuoglu E. Comparison of three back-propagation training algorithms for two case studies. Indian Journal of Engineering and Materials Science. 2005;**12**:434-442

[26] Komjathy A. Global ionospheric total electron content mapping using the Global Positioning System [PhD Thesis]. New Brunswick, Canada: Department of Geodesy and Geomatics Engineering Technical Report No. 188, University of New Brunswick, Fredericton; 1997

[27] Richmond A, Emmert J, Nair M, Maus S, Woods A, Wickwar V, Barnes R, Maute. Apex Coordinate Conversion Utility [Internet]. 2011. Available from: http://www.ngdc.noaa.gov/geomag/geom_util/apex.shtml [Accessed: 2016-11-20]

[28] Okoh D. Computer Neural Networks on MATLAB. North Charleston, SC, USA: Cre-atespace; 2016. p. 52. ISBN-13: 978-1539360957

[29] Gulyaeva TL, Huang X, Reinisch BW. Plasmaspheric extension of topside electron den-sity profiles. Advances in Space Research. 2002;**29**(6):825-831

[30] Gulyaeva TL, Bilitza D. Towards ISO standard earth ionosphere and Plasmasphere model. In: Larsen RJ, editor. New Developments in the Standard Model. Hauppauge, New York, USA: Nova Science Publishers; 2012. pp. 1-39

[31] Hochegger G, Nava B, Radicella SM, Leitinger R. A family of ionospheric models for different uses. Physics and Chemistry of the Earth. 2000;**25**(4):307-310

[32] Radicella SM, Leitinger R. The evolution of the DGR approach to model electron density profiles. Advances in Space Research. 2001;**27**:35-40. DOI: 10.1016/S0273-1177(00)00138-1

[33] Nava B, Coïsson P, Radicella SM. A new version of the NeQuick ionosphere electron density model. Journal of Atmospheric and Solar - Terrestrial Physics. 2008;**70**(15):1856-1862

[34] Bilitza D, Reinisch BW. International reference ionosphere 2007: Improvements and new parameters. Advances in Space Research. 2008;**42**(4):599-609

[35] Nava B, Radicella SM. The NeQuick Model: Characteristics and Uses. In: IGS Workshop. Pasadena; 23-27 June 2014